

M87 X-RAY VARIABILITY

NASA Grant NAG5-4830

Final Report

For the Period 1 July 1997 through 30 October 1999

Principal Investigator
Dr. Daniel E. Harris

June 2000

Prepared for:

National Aeronautics and Space Administration
Goddard Space Flight Center
Greenbelt, Maryland 20771

Smithsonian Institution
Astrophysical Observatory
Cambridge, Massachusetts 02138

The Smithsonian Astrophysical Observatory
is a member of the
Harvard-Smithsonian Center for Astrophysics

The NASA Technical Officer for this grant is Robert Petre, 662.0, NASA/Goddard Space
Flight Center, Greenbelt, MD 20771

This image shows a single sheet of white paper with horizontal blue or grey ruling lines. The lines are evenly spaced and run across the width of the page. There are no margins, text, or other markings on the paper.

| | | | |
|------------------------|--|-------------------------|--|
| 1. Name of the vessel | | 2. Date of departure | |
| 3. Name of the captain | | 4. Name of the master | |
| 5. Name of the vessel | | 6. Name of the vessel | |
| 7. Name of the vessel | | 8. Name of the vessel | |
| 9. Name of the vessel | | 10. Name of the vessel | |
| 11. Name of the vessel | | 12. Name of the vessel | |
| 13. Name of the vessel | | 14. Name of the vessel | |
| 15. Name of the vessel | | 16. Name of the vessel | |
| 17. Name of the vessel | | 18. Name of the vessel | |
| 19. Name of the vessel | | 20. Name of the vessel | |
| 21. Name of the vessel | | 22. Name of the vessel | |
| 23. Name of the vessel | | 24. Name of the vessel | |
| 25. Name of the vessel | | 26. Name of the vessel | |
| 27. Name of the vessel | | 28. Name of the vessel | |
| 29. Name of the vessel | | 30. Name of the vessel | |
| 31. Name of the vessel | | 32. Name of the vessel | |
| 33. Name of the vessel | | 34. Name of the vessel | |
| 35. Name of the vessel | | 36. Name of the vessel | |
| 37. Name of the vessel | | 38. Name of the vessel | |
| 39. Name of the vessel | | 40. Name of the vessel | |
| 41. Name of the vessel | | 42. Name of the vessel | |
| 43. Name of the vessel | | 44. Name of the vessel | |
| 45. Name of the vessel | | 46. Name of the vessel | |
| 47. Name of the vessel | | 48. Name of the vessel | |
| 49. Name of the vessel | | 50. Name of the vessel | |
| 51. Name of the vessel | | 52. Name of the vessel | |
| 53. Name of the vessel | | 54. Name of the vessel | |
| 55. Name of the vessel | | 56. Name of the vessel | |
| 57. Name of the vessel | | 58. Name of the vessel | |
| 59. Name of the vessel | | 60. Name of the vessel | |
| 61. Name of the vessel | | 62. Name of the vessel | |
| 63. Name of the vessel | | 64. Name of the vessel | |
| 65. Name of the vessel | | 66. Name of the vessel | |
| 67. Name of the vessel | | 68. Name of the vessel | |
| 69. Name of the vessel | | 70. Name of the vessel | |
| 71. Name of the vessel | | 72. Name of the vessel | |
| 73. Name of the vessel | | 74. Name of the vessel | |
| 75. Name of the vessel | | 76. Name of the vessel | |
| 77. Name of the vessel | | 78. Name of the vessel | |
| 79. Name of the vessel | | 80. Name of the vessel | |
| 81. Name of the vessel | | 82. Name of the vessel | |
| 83. Name of the vessel | | 84. Name of the vessel | |
| 85. Name of the vessel | | 86. Name of the vessel | |
| 87. Name of the vessel | | 88. Name of the vessel | |
| 89. Name of the vessel | | 90. Name of the vessel | |
| 91. Name of the vessel | | 92. Name of the vessel | |
| 93. Name of the vessel | | 94. Name of the vessel | |
| 95. Name of the vessel | | 96. Name of the vessel | |
| 97. Name of the vessel | | 98. Name of the vessel | |
| 99. Name of the vessel | | 100. Name of the vessel | |

See attached the following two papers:

1. X-ray Variability in M87 (D.E. Harris, J.A. Biretta, and W. Junor) MNRAS, 284, L21, 1997.
2. X-ray Variability in M87: 1992 - 1998 (D.E. Harris, J.A.j Biretta, and W. Junor) in "The Radio Galaxy Messier 87: proceedings of a workshop held at Schloss Ringberg, Germany, 15-19 September 1997", Springer-Verlag Lecture Notes in Physics Vol. 530, H.-J. Roeser and K. Meisenheimer, ed., p.319, 1999.

Hermann-Josef Röser
Klaus Meisenheimer (Eds.)

The Radio Galaxy Messier 87

Proceedings,
Schloss Ringberg,
Germany 1997



Springer

- Reynolds C. S., Fabian A. C., Celotti A., Rees M. G., 1996, MNRAS, 283, 873
 Reynolds C. S., Inayama K., Crawford C. S., Fabian A. C., 1998, MNRAS, submitted
 Shakura N. I., Sunyaev R. A., 1973, A&A, 24, 337
 Stone J. M., Hawley J. F., Gammie C. F., Belbus S. A., 1996, ApJ, 463, 656
 Zirbel E. L., Baum S. A., 1995, ApJ, 448, 521

X-ray Variability in M87: 1992 – 1998

D. E. Harris¹, J. A. Biretta², and W. Junor³

¹ Smithsonian Astrophysical Observatory
 60 Garden St.

Cambridge, MA 02138, USA

² Space Telescope Science Institute
 3700 San Martin Dr.

Baltimore, MD 21218, USA

³ University of New Mexico
 800 Yale Blvd. NE

Albuquerque, NM 87131, USA

Abstract. Beginning in 1995 June, we have obtained an observation of M87 with the ROSAT High Resolution Imager (HRI) every 6 months. We present the measurements of X-ray intensity for the core and knot A through 1998 January. We find significant changes in both components. For the core, intensities measured in June 1995, December 1996, and December 1997 are roughly 30% higher than values obtained at three intervening times. For knot A, a secular decrease of approximately 15% is interrupted only by an intensity jump (3σ) in December 1997. Because the background used for subtraction is probably underestimated, we suspect the actual variation is somewhat greater than these values indicate.

1 Introduction

The initial results of our X-ray monitoring of M87 (Harris, Biretta, and Junor (1997), HBJ hereafter) were based on a re-analysis of two Einstein Observatory HRI observations, a ROSAT archival HRI pointing in June 1992, and the first two of our ongoing series of an observation every 6 months (June and December 1995). There we demonstrated that the core was variable at the 15% level and that knot A showed a gradual decline in intensity. In this paper we include data from 4 additional observations, with the most recent consisting of two segments: December 14, 1997 (8 ksec) and January 5, 1998 (20.6 ksec). We have also re-measured some of the earlier data to ensure that all data were treated uniformly.

2 Review of Problems and Measuring Techniques

There are three known problems affecting accurate photometry of ROSAT HRI data. The first is that the core and knot A (the two brightest features which we can measure with a 30 ksec observation) are separated by only

complex emission distribution (Harris, Biretta, and Junor (1999)), thereby making it difficult to estimate the surface brightness that would have been observed at the locations of the core and knot A if they were absent.

The most serious problem however, is the image degradation which means that the effective point response function (PRF) is widened and distorted from its quasi-Gaussian shape ($\text{FWHM} \approx 5.5''$) to an irregular distribution with FWHM of $7''$ to $10''$. The degradation is caused by bad aspect solutions; sometimes associated with the spacecraft wobble and occasionally to time segments for which the aspect solution can be up to $10''$ (or more) away from the primary solution. This situation means that we have no assurance that our standardized measuring areas contain the same fraction of total source counts for each observation.

To mitigate the severity of these problems, we made two separate measurements. For the first, we take the ratio of net counts in circular apertures ($r=6''$) centered on the core and knot A. To first order, we expect that the effective PRF will be the same for these close sources. Consequently the major error of this approach is that we will measure different fractions of the total source counts in different observations. Since the background correction uses a region with a slightly lower surface brightness than that found adjacent to the core and knot A, the non-variable background component will increasingly dilute any variable feature as the effective PRF gets larger; i.e. fewer photons from the unresolved component will remain within the small measuring aperture.

The second measurement utilizes two adjacent rectangles rotated by 20° . Each rectangle is $16''$ by $26''$ with their common border ($26''$) perpendicular to the line joining the core and knot A, and centered on the 'reference point'. The reference point is halfway between the core and knot A. Surrounding these two rectangles is the background 'frame' which is $10''$ wide. This background frame is used both for the circular and rectangular measurements. The geometry is depicted in Fig. 2 of HBJ. The larger area of the rectangle compared to the small circle is designed to include most of the source counts even when there is substantial degradation of the PRF. However, since it will include more of the non-variable background, the actual variability should be somewhat greater than that found by this technique.

As a control, we also measure the net counts in a circular aperture ($r=12''$) centered $45''$ to the SE of the reference point ($\text{PA}=110^\circ$). This location is on a plateau in the X-ray brightness distribution. Since we use the same background frame as for the other measurements, the resulting value is always negative.

Finally, to accommodate any changes in quantum efficiency we employed a 'self-calibration' by measuring the count rate of the bright part of the cluster gas within a large circle with radius $276''$, but excluding the adjacent rectangles containing the core and knot A. For this measurement, we used a background annulus with radii of $280''$ and $300''$. All measured net count

rates were then multiplied by a correction factor (always 5% or less) to give the cluster gas net count rate would be the same as that for our observation of June 1995.

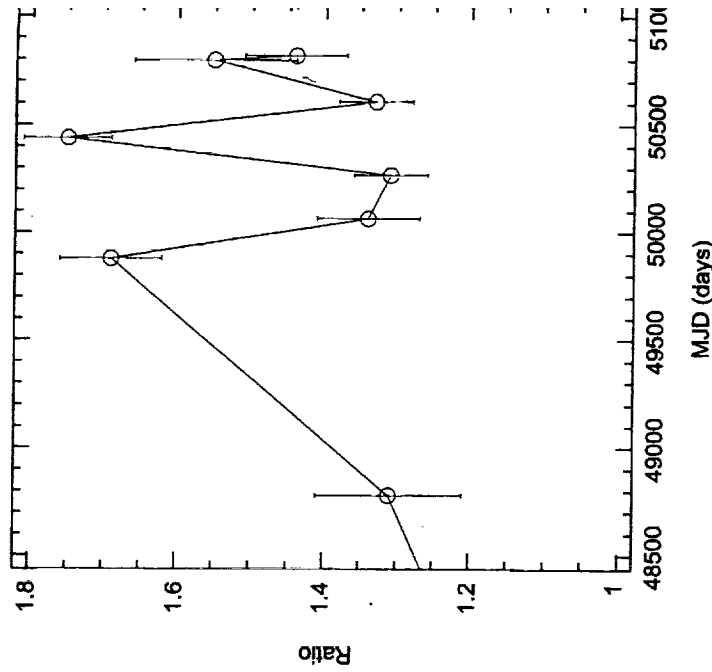


Fig. 1. The ratio of the core to knot A. Values are the ratio of net counts in circular apertures with radius of $6''$.

3 Results

The measured values are shown in Fig. 1 (the ratios) and 2 (the counts). It can be seen that the major features of the ratio plot mimic the count rate variability for the core. This is consistent with expectations that the count rate will be more variable than knot A. The decrease in the intensity of the cluster gas following the observation of June 1995 ($\text{MJD} = 49876$) coincides with the decrease observed with the HST between MJD 49840 and MJD 49900 (Fig. 3 of Tsvetanov et al. (1999)).

In Biretta, Stern, and Harris (1991), we analyzed the Einstein X-ray emission from knot A and argued that the X-ray emission from knot A was most likely syn-

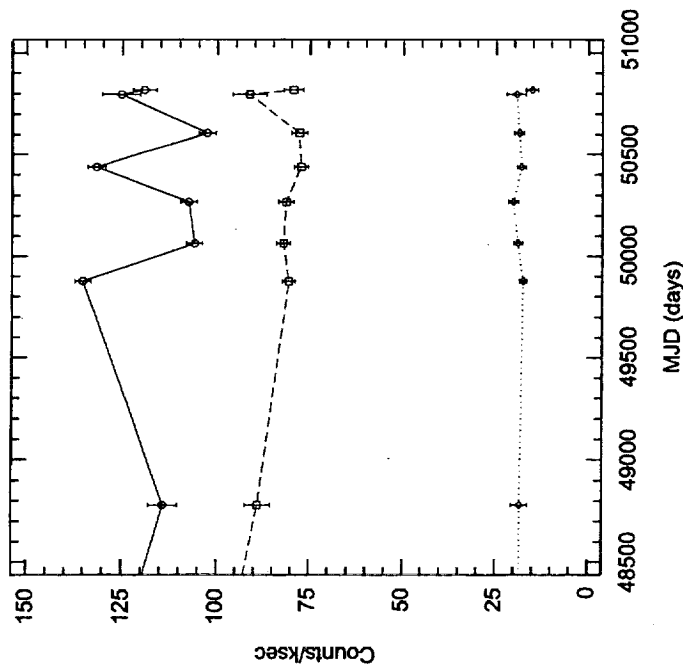


Fig. 2. The net count rates for the core, knot A, and a control region. The solid line is for the core, the dashed line is for knot A, and the control circle values are connected with a dotted line. Note that the control region is the net counts in a circle $45''$ SE of the reference point, with the background from the frame. Therefore all control values are negative, but are plotted here as positive numbers. Thus the small apparent drop for the last measurement is actually in the opposite sense from those of the core and knot A. The lines running off the left side of the figure connect to the Einstein values (HBJ).

emission rather than thermal bremsstrahlung or inverse Compton emission. For a magnetic field strength of $\approx 200 \mu\text{G}$ (the minimum pressure field), we found that electrons with Lorentz energy factors, γ , of 2×10^7 were required and typical half lives were of order ten years. The observed decrease of knot A (Fig. 2) is consistent with these estimates, but we do not yet understand why only a small fraction of shocks produce enough $\gamma = 10^7$ electrons to generate an X-ray intensity detectable with current technology. We suspect that even the knot A shock (≈ 70 pc across as measured at radio and optical wavelengths) is not a uniform single entity, but may well display a complex brightness distribution at the highest energies where synchrotron losses are severe. Thus we expect that higher resolution X-ray observations will show occasional bright, compact components which will not persist many years

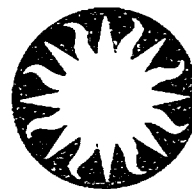
(e.g. Biretta et al. (1999) find optical features with these character the December 1997 increase in knot A is real, it could represent emission such a feature. AXAF observations have been proposed to obtain 8 exposures with the High Resolution Camera.

References

- Biretta, J.A., Stern, C.P., and Harris, D.E. (1991): The Radio to X-ray of the M 87 Jet and Nucleus, *AJ* 101, 1632-1646
 Biretta, J.A. et al. (1999) (this volume): *Ringberg Workshop on M 87* (Berlin, Heidelberg)
 Harris, D.E., Biretta, J.A., and Junor, W. (1997): X-ray Variability in M 87, *RAS* 284, L21-L27
 Harris, D.E., Biretta, J.A., and Junor, W. (1999) (this volume): *Ringberg Workshop on M 87* (Springer, Berlin, Heidelberg)
 Tsvetanov, Z.I., Hartig, G.F., Ford, H.C., Kriss, G.A., Dopita, M.A., L.L., and Harms, R.J. (1999) (this volume): The Nuclear Spectrum of M 87, *Ringberg Workshop on M 87* (Springer, Berlin, Heidelberg)



Harvard-Smithsonian Center for Astrophysics



Preprint Series

No. 4458

(Received December 12, 1996)

X-RAY VARIABILITY IN M87

D.E. Harris

Smithsonian Astrophysical Observatory

J.A. Biretta

Space Telescope Science Institute

and

W. Junor

University of New Mexico, Institute for Astrophysics

To appear in

Monthly Notices of the Royal Astronomical Society

Center for Astrophysics
Preprint Series No. 4458

X-RAY VARIABILITY IN M87

D.E. Harris
Smithsonian Astrophysical Observatory

J.A. Biretta
Space Telescope Science Institute

and

W. Junor
University of New Mexico, Institute for Astrophysics

X-ray variability in M87

D. E. Harris

SAO MS-3, 60 Garden St., Cambridge MA 02138 USA

harris@cfa.harvard.edu

J. A. Biretta

STScI, 3700 San Martin Dr., Baltimore MD 21218 USA

biretta@stsci.edu

W. Junor

The Institute for Astrophysics, Dept. of Physics and Astronomy, Univ. of New Mexico,

800 Yale Blvd., NE Albuquerque, NM 87131 USA

bjunor@astro.phys.unm.edu

Received 1996

ABSTRACT

We present the evidence for X-ray variability from the core and from knot A in the M87 jet based on data from two observations with the Einstein Observatory High Resolution Imager (HRI) and three observations with the ROSAT HRI. The core intensity showed a 16% increase in 17 months ('79-'80); a 12% increase in the 3 years '92 to '95; and a 17% drop in the last half of 1995. The intensity of knot A appears to have decreased by 16% between 92Jun and 95Dec. Although the core variability is consistent with general expectations for AGN nuclei, the changes in knot A provide constraints on the x-ray emission process and geometry. Thus we predict that the x-ray morphology of knot A will differ significantly from the radio and optical structure.

Key words: galaxies:active - galaxies:individual:M87 - galaxies:jet - X-rays:galaxies

1 INTRODUCTION

The Einstein Observatory (EO) HRI observations of M87 were the first to clearly isolate X-ray emission of the core of the galaxy and of the brightest knot in the jet from the broader distributions known previously (Schreier, Gorenstein & Feigelson 1982). These authors suggested that the core emission was resolved, and thus likely to be thermal bremsstrahlung whereas the emission from knot A was probably synchrotron emission. The EO data were further analyzed by Biretta, Stern & Harris 1991 (hereafter 'BSH'), who summed the two EO/HRI observations and selected only a portion of the data in order to achieve the best possible image integrity. BSH argued that most of the core emission was unresolved and thus could be similar to nuclear emission from other AGN. Since AGN exhibit X-ray variability with timescales of days to years (e.g. Mushotzky, Done & Pounds 1993), the same behavior could occur in M87.

When the ROSAT archival data became publicly available, it was evident that the intensity ratio of the core to knot A had changed, and we thus proposed further observations with the ROSAT HRI. In this paper we report only on the gross intensity changes since poor aspect solutions (which have an effect similar to 'pointing jitter') have degraded the effective resolution of the 1995 data. Consequently, the sizes of the regions used to measure fluxes contain a higher percentage of background emission than desirable. Despite these difficulties, we find convincing evidence for variability in both the core (+ knot D) and in knot A (+ knot B).

The most reliable evidence for variability comes from a comparison between the multiple observations made with each satellite. When comparing Einstein and ROSAT data however, the difference in effective area as a function of energy between the two satellites introduces an uncertainty because we have no knowledge of the X-ray spectral distributions of the various components.

2 DATA REDUCTION

2.1 The data

The observations used in this paper are summarized in Table 1. The ROSAT images are shown in Figure 1, and may be compared to Figures 1 and 2 of BSH. It is apparent that the 1995 data suffer from severe aspect smearing and that the intensity ratio of the core to knot A has increased. The degradation in resolution from the aspect problem is not easily fixed. The only other source in the field with a reasonable intensity is too far off axis ($12.2''$) to serve as a template for a point response function.

2.2 Selection of regions for measuring the intensities

To derive reliable intensities, we need to ensure that we collect the same fraction of source counts for each feature and each observation. Poor aspect degrades the resolution. N/S profiles on the maps smoothed with a $3''$ Gaussian give FWHMs of $7.5''$ for the core and $7.2''$ for knot A in the 92Jun data, but $10.0''$ for both features in the 95Jun data. Therefore, small radii circles would not measure the same fraction of counts for different observations.

Although larger integration areas can overcome the aspect smearing, they will suffer from greater contamination with (non-variable) background emission. Moreover, the core and knot A are separated by only $12''$. Consequently, we have made two sets of intensity measurements: one by selecting adjoining boxes, and the other with circular apertures of radius, $r=6''$. The former will be used for comparing countrates but will underestimate any variability because of contamination by extended, non-variable emission. The latter method should be more reliable for measuring the ratio of the core to knot A (assuming the aspect smearing affects both components equally), but cannot be used for comparing countrates for a given feature from different observations.

For the ‘adjoining rectangle’ method, we chose in each map the same central reference point lying on the line joining the two peaks, at about the location of the saddle point in X-ray brightness between the core and knot A. This reference point was derived from the $3''$ smoothed contour plots. Using a rotation of 20° , two adjoining boxes of dimensions $\Delta x' = 16''$, $\Delta y' = 26''$ were constructed. (The primed coordinates refer to the rotated frame.) For the background, we joined the two measuring boxes to make the sum ($32'' \times 26''$) and used a $10''$ border around this box (all centered on the reference point). We also use this same background frame for the $r=6''$ circular aperture. A rough sketch of this geometry is shown in Figure 2.

For each map, positions of the core and knot A were determined by the detection algorithm in IRAF/PROS and checked with contour diagrams of the smoothed images (Fig. 1). For the circular apertures, these positions defined the centers of the circles. The two Einstein observations were reduced in the same manner as the ROSAT data.

3 VARIABILITY OF THE CORE AND KNOT A

3.1 Ratio of core to knot A

The observable which is least affected by systematic differences between EO and ROSAT, and between differences in quality of aspect solutions, is the ratio of the flux of the core to knot A. While there will always be some degree of ‘contamination’ in the measuring circles because the background is estimated within a region somewhat removed from the core and knot A, this effect is minimized by using the small area of the circular apertures. We also expect that whatever loss occurs from aspect smearing will affect both core and knot A equally, so such an effect will only serve to reduce any real changes in the ratio.

The only important uncertainty which we have identified is the difference in the effective areas of EO and ROSAT. If the core were significantly harder than knot A, then EO would find a different ratio for the core to knot A than would ROSAT, supposing that they observed the source at the same time. The unknown spectral distributions of the core and knot A lead to an uncertainty of roughly $\pm 25\%$ (for a reasonable range of spectral distributions, see below) when comparing EO with ROSAT countrates. The results for the circular apertures and ratios are given in Table 2 and plotted in Figure 3a.

3.2 Countrates for the core and knot A

While the HRI on Einstein was very similar to that on ROSAT, the quantum efficiency and effective area were much smaller and the energy band was wider. Both the PIMMS software (a multi-mission tool distributed by the High Energy Astrophysics Science Archive Research Center, Goddard Space Flight Center) and the 'xflux' task in IRAF/PROS use the appropriate effective areas of mirror/detector pairs, and allow convolution with simple spectral shapes. The conversion factor, C , ($\text{ROSAT c/s} = C \times \text{EO c/s}$) for a power law spectrum with energy index $\alpha = 1.3$ [$S \propto \nu^{-\alpha}$] and column density, $\log N_H = 20.38$ (the values used in BSH), is 1.75 for PIMMS and 2.05 for xflux. These numbers may be compared to conversion factors deduced from Table 4 of the HRI Calibration Report (David et al. 1995) for various supernova remnants where the conversion factors are generally greater than 3. In view of this uncertainty, we have chosen to use the M87 cluster gas itself as our primary intensity calibrator. To do this, we measured the countrate in a circle of radius $276''$ centered on the reference point described above. For the background, we used an annulus with radii of $280''$ and $300''$. We excluded from the circle the inner box ($32'' \times 26''$, rotated by 20°) which contains the core and knot A. The correction factors necessary to obtain the 95Jun value (which is taken as the fiducial point) are listed in Table 3. They may be compared with results for bremsstrahlung spectra with $kT = 2$ keV and $\log N_H = 20.38$ of 2.1 for PIMMS and 2.45 for xflux.

As discussed above, we have based our countrate estimates on intensity measurements in $16'' \times 26''$ boxes. The countrates for the core and knot A from both instruments are given in Table 4 and plotted in Figure 3b. The chief uncertainty is the correction factor used to convert Einstein countrates to ROSAT values. This factor is derived from the countrates of the cluster gas which is believed to have a temperature close to 2 keV (Fabricant, Lecar & Gorenstein 1980; Nulsen & Böhringer, 1995). Consequently, the conversion factor could be as much as 35% smaller if the spectral distribution of the core or knot A were to be extremely different from that of the cluster gas. This spectral uncertainty precludes a definitive statement about the history of the variability on the 10 year time scale covered by the Einstein and ROSAT observations. However, the Einstein data alone show that the core intensity increased by 16% (4σ) between 79Dec and 80Jul whereas knot A increased by less than 7% during the same period (1.5σ). During the 3.5 year ROSAT coverage, knot A declined by 16% and the core increased by 12% (3σ) from 92Jun to 95Jun and declined by 17% (7σ) in the following 6 months.

We also searched for short time-scale variability during each ROSAT observation (one to three days of length). Kolmogorov-Smirnov and Cramer-von Mises one-sample goodness-of-fit tests were performed using the circular apertures for both the core and knot A in order to test the null hypothesis of constant source intensity. The only instance where the statistic exceeded 99% was for knot A, 95Jun. The light curve shows a 20% enhancement for about 12 hours on 95Jun09. This behavior could be caused by aspect problems, and will be investigated at a later time.

4 DISCUSSION

The magnitude of the characteristic changes is of order $0.02 \text{ counts s}^{-1}$. The conversion of ROSAT countrate to luminosity at M87 (assumed to be 16 Mpc distant) varies between $3 \times 10^{41} \text{ erg/count}$ for soft spectral distributions (power laws with $\alpha = 2.5$ or bremsstrahlung spectra with $kT = 0.2 \text{ keV}$) to $14 \times 10^{41} \text{ erg/count}$ for harder spectra ($\alpha = 0.2$ or $kT = 10 \text{ keV}$). Consequently, the changes we have observed are of order $\Delta L_x(0.5\text{--}3\text{keV}) = 10^{40} \text{ erg/s}$; substantially larger than the typical luminosities of galactic binaries (Tanaka & Lewin 1995; van Paradijs & McClintock 1995).

Conventional explanations for the X-ray emission from the cores of galaxies containing massive black holes are either thermal emission from the putative accretion disk or non-thermal emission, possibly associated with the inner jet, which may be strongly beamed. Either of these models can easily accommodate the observed variability and short timescales. Additionally, larger fractional changes have been observed for other AGN (e.g. the Seyfert I galaxies reported by Boller, Brandt & Fink 1996). Rapid variations have also been seen in VLBI observations of the nucleus. Junor & Biretta (1995) have found evidence for changes in the jet structure in 1.3 cm VLBI images on very small scales ($\approx 0.01 \text{ pc}$) accompanied by a decrease in the core brightness of $\approx 30\%$ over 5 months in 1992. In 1977, a ‘flare’ was observed with 2.3 GHz VLBI; the amplitude changed by 30% over 4 months (Morabito, Preston & Jauncey 1988). While there are no simultaneous flux measurements in the radio or optical bands, the sporadic data which are available show the same sort of behavior as that in Figure 3b. The 2 cm radio core flux density ($0.15''$ resolution) increased by 13% between 93Jan and 94May. (These VLA data are described in Biretta, Zhou & Owen (1995).) The ultraviolet flux from the core ($0.04''$ resolution) decreased by a similar amount between 94Aug and 95Jul (Biretta, Sparks & Macchetto 1996). These data are consistent with a maximum in the core’s lightcurve occurring in mid 1994.

For knot A, the situation is different. Even if the apparent decrease of more than 10% between 1980 and 1992 is uncertain because the spectral distribution is unknown, the secular dimming of 16% between 1992Jun and 1995Dec is a 3σ effect. The observed decline (of order 4%/yr) is consistent with the halflife (12.8 yr) estimated by BSH for relativistic electrons producing X-ray synchrotron emission in a $200\mu\text{G}$ field. However, the physical size of knot A is known from radio and optical data to be of order 70 parsec by a few parsecs (i.e. a thin shock disk). Therefore, the observed decrease could be explained by (a) 100% variability from a region of order a light year across which, at maximum, contributes about 20% of the knot A flux; (b) the entire X-ray emitting volume of knot A could be substantially smaller than the diameter of the disk which produces the optical and radio emission; or (c) relativistic effects such as a change of a beaming angle might be present. For the former cases, the time scale of the observed decrease favors synchrotron emission as the X-ray emission process. BSH estimate cooling times for thermal models of over 100,000 years, and inverse Compton models always involve relativistic electrons with substantially lower energies (and hence longer lifetimes) than those required to produce X-ray synchrotron emission. Additional ROSAT observations have been approved to monitor M87 at 6 month intervals and contemporary optical and radio observations are planned.

ACKNOWLEDGMENTS

Reduction of ROSAT data at SAO was supported by NASA contract NAS5-30934 and NASA grant NAG5-2957 provided partial support of DEH and JAB. J. D. Silverman performed the Einstein measurements. We thank several of our colleagues at the CfA for assistance in understanding the change in the EINSTEIN HRI sensitivity and the referee, A. Edge, who made several useful suggestions for improving the manuscript.

REFERENCES

- Biretta J.A., Stern C.P., Harris D.E., 1991, *AJ*, 101, 1632
Biretta J.A., Zhou F., Owen F.N., 1995, *ApJ*, 447, 582
Biretta J.A., Sparks W.B., Macchetto F. 1996, in preparation
Boller Th., Brandt W.N., Fink H., 1996, *A&A*, 305, 53
David L.P., Harnden Jr. F.R., Kearns K.E., Zombeck M.V., 1995, "The ROSAT HRI Calibration Report", available from RSDC MS-3, SAO, Cambridge, MA 02138, USA, and via WWW: http://hea-www.harvard.edu/rosat/rsdc_www/HRI-CAL-REPORT/hri.html
Fabricant D., Lecar M., Gorenstein P., 1980, *ApJ*, 241, 552
Junor W., Biretta J. A., 1995, *AJ*, 109, 500
Morabito D.D., Preston R.A., Jauncey D.L., 1988, *AJ*, 95, 1037
Mushotzky R.F., Done C., Pounds K.A., 1993, *ARA&A*, 31, 717
Nulsen P.E.J., Böhringer H., 1995, *MNRAS*, 274, 1093
Schreier E.J., Gorenstein P., Feigelson E.D., 1982, *ApJ*, 261, 42
Tanaka Y., Lewin W.H.G., 1995, in Lewin W.H.G., van Paradijs J., van den Heuvel E. P. J., eds, *X-ray Binaries*, Cambridge Univ. Press, Cambridge, p.126
van Paradijs J., McClintock J.E., 1995, in Lewin W.H.G., van Paradijs J., van den Heuvel E. P. J., eds, *X-ray Binaries*, Cambridge Univ. Press, Cambridge, p.58

Table 1 Observations

| Date | Seq # | Livetime (secs) | Comments |
|-----------|----------|--------------------|---------------------|
| 1979Jul05 | H282 | 72662 | See BSH for details |
| 1980Dec09 | H10316 | 49249 | See BSH for details |
| 1992Jun07 | wh700214 | 13954 | good aspect |
| 1995Jun09 | us701712 | 44264 | poor aspect |
| 1995Dec16 | us701713 | 40362 | poor aspect |

Notes: Deadtimes for Einstein are assumed to be 4%; for ROSAT they are 2%.

Table 2 Circular Aperture Counts for the Ratio of Core / Knot A

| | 1979 | 1980 | 1992Jun | 1995Jun | 1995Dec |
|-------------|------------|------------|------------|------------|------------|
| core raw | 2185 | 1535 | 1281 | 4465 | 3267 |
| core net | 1842 (48) | 1325 (40) | 1084 (37) | 3843 (68) | 2702 (58) |
| knot A raw | 2082 | 1383 | 1022 | 2892 | 2578 |
| knot A net | 1742 (47) | 1174 (38) | 826 (33) | 2271 (55) | 2012 (52) |
| ratio (net) | 1.06 (.04) | 1.13 (.05) | 1.31 (.07) | 1.69 (.05) | 1.34 (.05) |

Note: 1σ errors are given in parentheses; those on the ratios are the sums of the errors on each component, taken in quadrature. The Einstein ratios may be compared to that derived in the BSH paper where extensive image processing was performed so that background contamination was minimized: $(\text{Core} + \text{knot D}) / (\text{knot A} + \text{knot B}) = 1.15$

Table 3 Intensity Calibration Based on Extended Thermal Emission

| Date | Raw (cnts) | Net countrate (c/s) | CorFac to 95Jun |
|-------|---------------|------------------------|-----------------|
| 79Jul | 124324 | 0.780 (0.010) | 2.940 (1.3%) |
| 80Dec | 72388 | 0.671 (0.012) | 3.418 (1.8%) |
| 92Jun | 57660 | 2.183 (0.034) | 1.050 (1.6%) |
| 95Jun | 185689 | 2.293 (0.019) | 1.000 (0.8%) |
| 95Dec | 167682 | 2.304 (0.020) | 0.995 (0.9%) |

Note: Raw counts are the value for the $r = 276''$ circle centered on the reference point, minus the counts in the rotated box ($32'' \times 26''$). The net countrate is based on the background subtraction of the $280''$ to $300''$ annulus. The 5% difference between 92Jun and 95Jun is ascribed to the change in high voltage (94Jun; see the HRI Calibration Report, David et al. 1995). The 16% difference between the two Einstein observations is reasonably close to the 12.3% drop in sensitivity expected in the 17 months between the two observations. This secular change in the sensitivity is scaled from the estimate of 8.7%/yr derived from observations of a number of supernova remnants and Abell 496 (Seward and Martenis, internal Einstein Memo of 1988 Jul 21). 1σ errors are given in parentheses.

Table 4 Core and Knot A Countrates

| Date | CORE | | KNOT A | |
|-------|---------------|---------------------------|---------------|---------------------------|
| | Box (cnts) | Net countrate (c/ksec) | Box (cnts) | Net countrate (c/ksec) |
| 79Jul | 4133 | 116.5 (2.8) | 3680 | 98.0 (2.6) |
| 80Dec | 2722 | 135.5 (3.8) | 2275 | 104.5 (3.5) |
| 92Jun | 2336 | 123.7 (3.9) | 1873 | 88.4 (3.5) |
| 95Jun | 8417 | 138.6 (2.2) | 5782 | 79.0 (1.8) |
| 95Dec | 6747 | 115.1 (2.1) | 5104 | 74.5 (1.9) |

Note: the box counts (columns 2 and 4) are given without any corrections but the countrates (columns 3 and 5) are corrected for background in the $10''$ wide frame and have been multiplied by the appropriate correction factor from Table 3. 1σ errors are given in parentheses.

Figure 1: Contour diagrams of the data with a 3'' FWHM Gaussian smoothing function. The maps have been scaled by $10^6/\text{lifetime}$ to change the units to counts/pixel/Megasec. The pixel size is 0.5'' and the contour levels are logarithmic: 40, 53, 70, 93, 124, 164, 218, and 290 c/pix/Ms. (a) 1992Jun; (b) 1995Jun; (c) 1995Dec.

Figure 2: A grey scale image of M87 with the approximate geometry for intensity measurements shown. The inner rectangle is divided into 2 equal areas for the 'adjoining rectangle' method discussed in the text.

Figure 3: Variability Results

For calendar dates, see Table 1. (a) the ratio of net counts in $r=6''$ circular apertures centered on the core and knot A. (b) the countrates (c/ksec) for the box measurements of the core (circles) and knot A (squares). The correction factors used are those from Table 3. Included as a control (the x's) are the differences between the countrates in the background frame and the countrates in a circle ($r=12''$) located $45''$ to the SE of the reference point (a region where the X-ray surface brightness is without large spatial gradients and is approximately 60% of the average frame value).

For the Einstein data, additional uncertainties caused by the unknown spectral distribution of components, are roughly +6% (for harder spectra, up to 10 keV, or α down to 0.3) and -35% (for softer spectra, down to 0.3 keV or α up to 2.4). Similar uncertainties would apply to the ROSAT data only if the variability was accompanied by a significant change in spectral distribution.

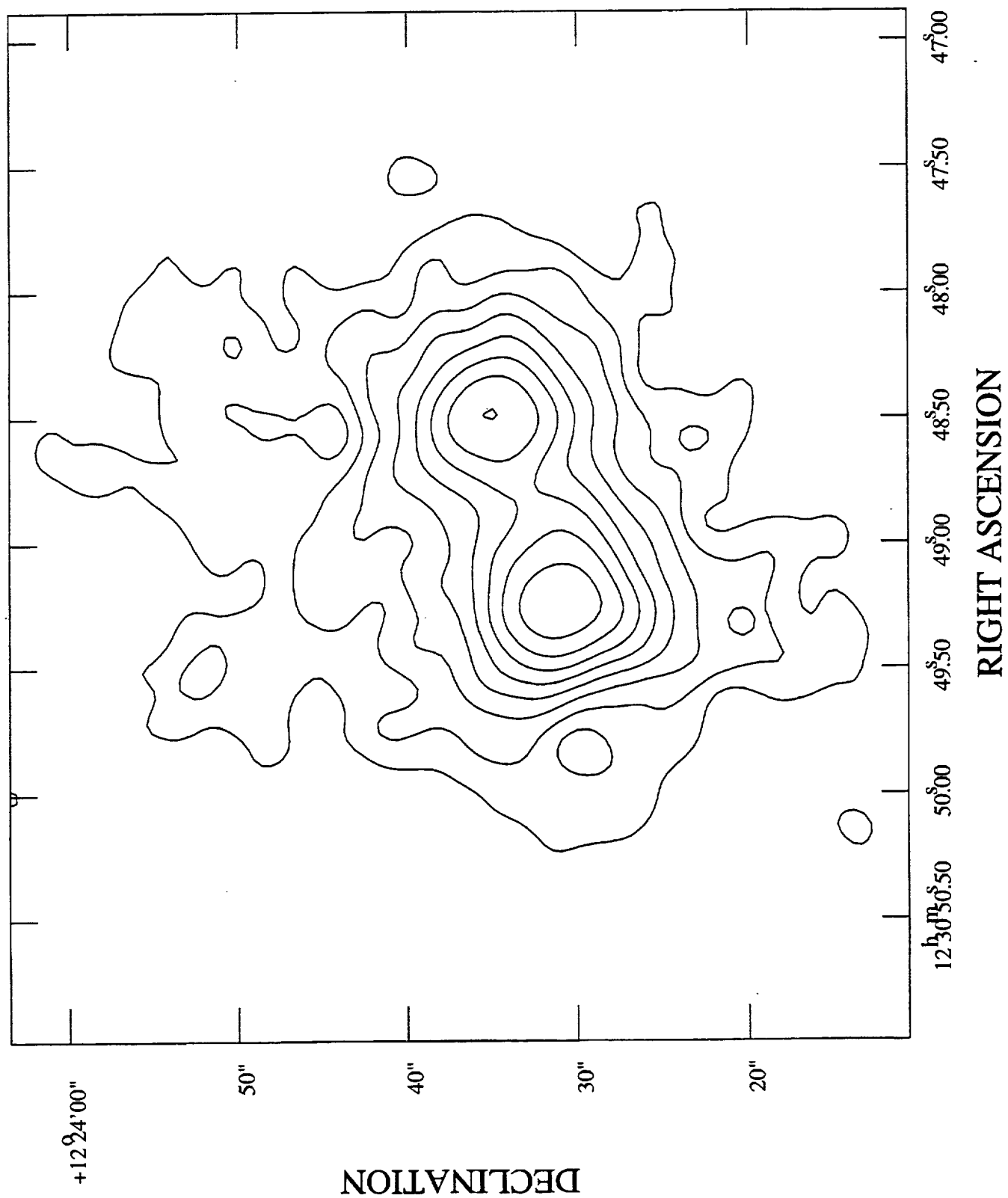


Fig 1a

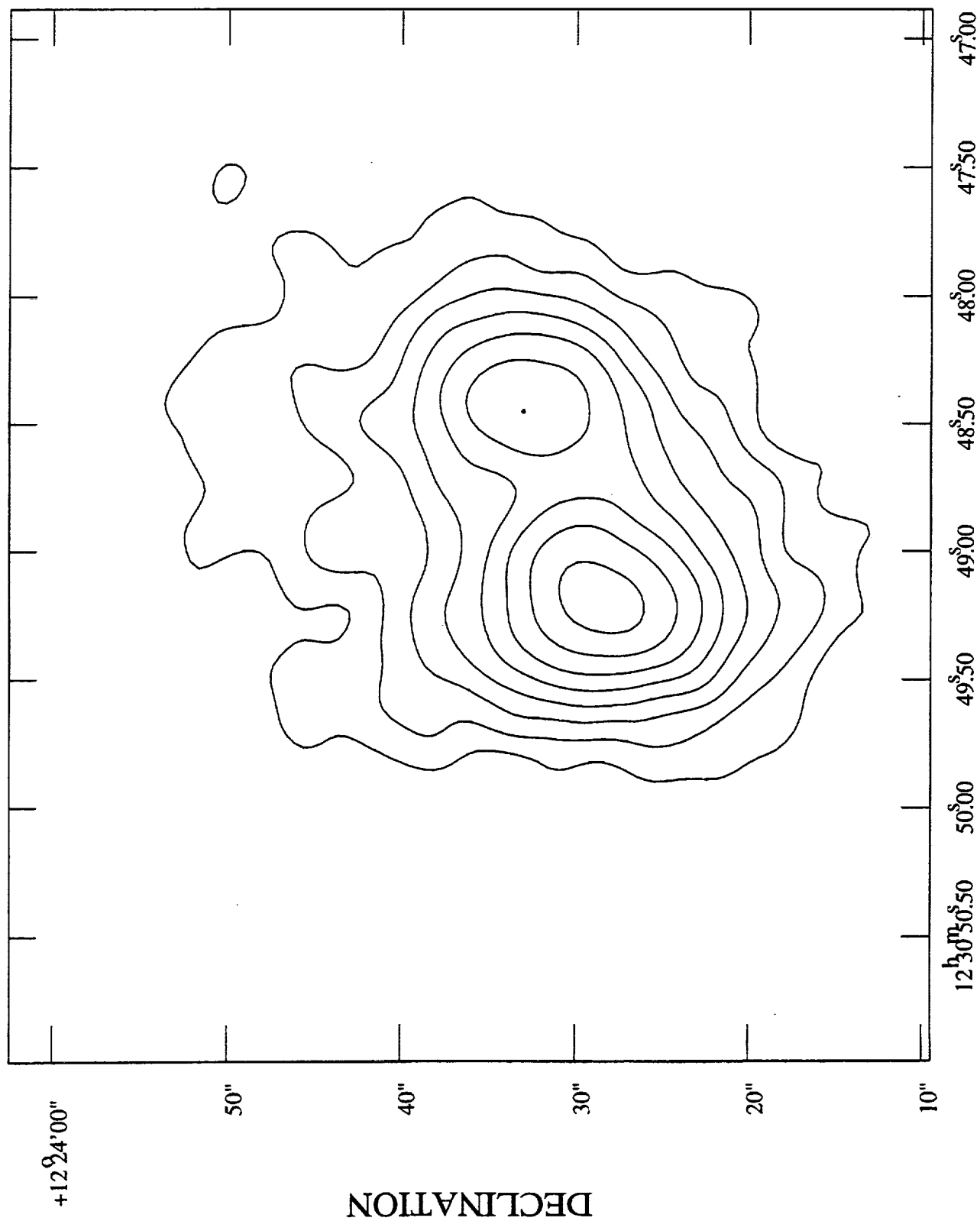


Fig 1 b.

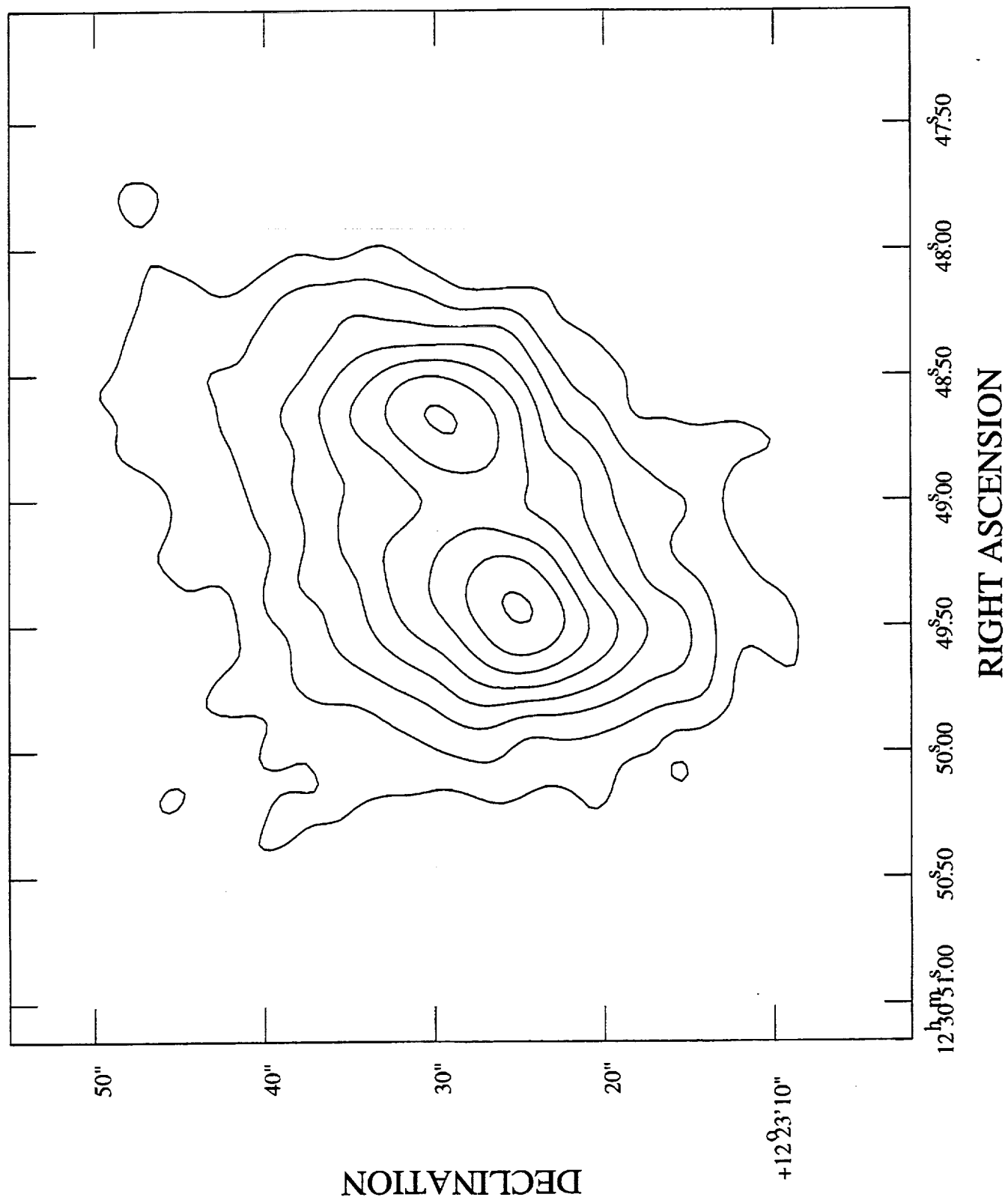


Fig 1c

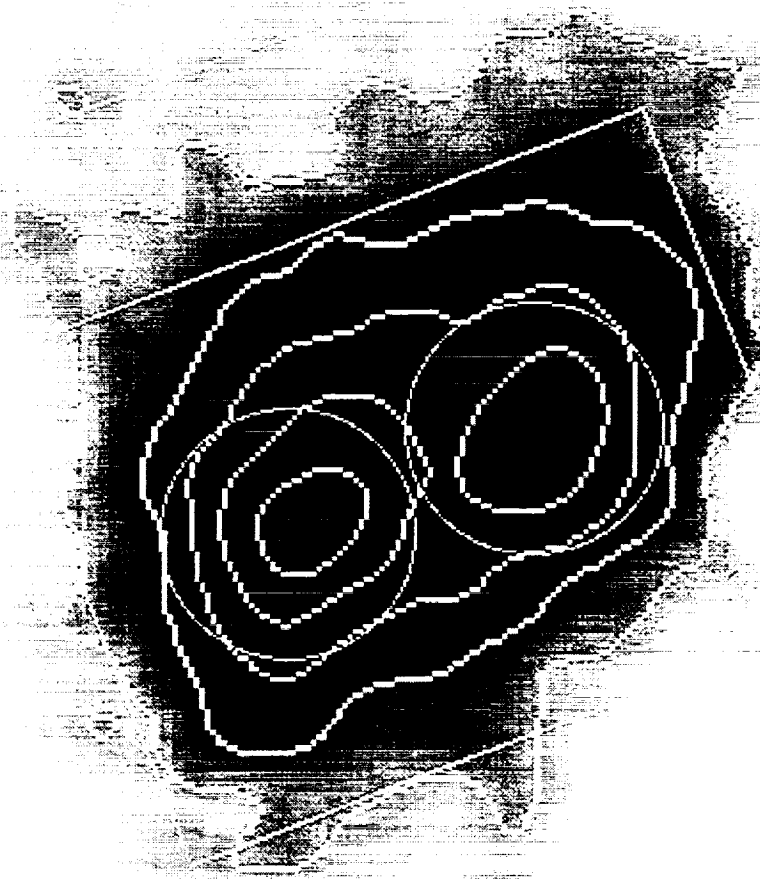


Fig 2

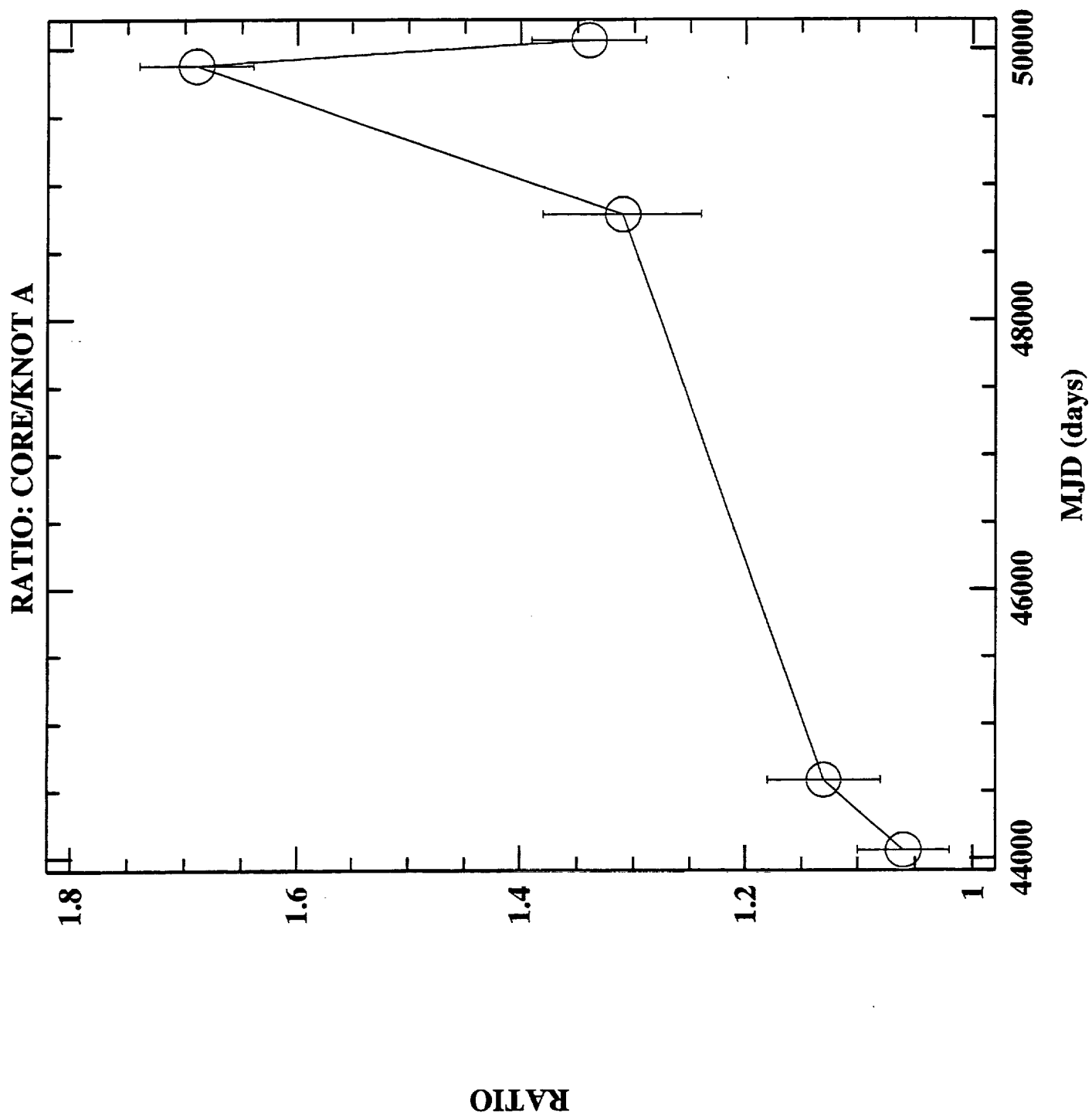


Fig 3a

